

NUMERICAL ANALYSIS OF THE THERMODYNAMIC EFFECT OF SPLITTER BLADES IN CENTRIFUGAL COMPRESSORS APPLIED FOR LOW REFRIGERATION CAPACITY

Rovanir Baungartner, baungartner@polo.ufsc.br

César J. Deschamps, deschamps@polo.ufsc.br

Programa de Pós-Graduação em Engenharia Mecânica

Universidade Federal de Santa Catarina

88040-900, Florianópolis, SC

Abstract. Centrifugal compressors are used for gas compression in several engineering applications. In the case of highly efficient centrifugal compressors, splitter blades are usually adopted as an alternative to increase the compressor mass flow rate. Nevertheless, currently the design of splitters is almost totally based on experience gathered from experimental data. The reason for the absence of clear design criteria is associated with the flow complexity in centrifugal impellers, which are dominated by three-dimensional viscous effects. The present study considers the numerical analysis of the flow through the first stage of a high speed centrifugal compressor, with the main purpose of verifying their effect on the compressor thermodynamic efficiency. Results for velocity and pressure fields are presented to help understand the main differences in performance originated by splitters.

Keywords: centrifugal compressor, splitter blades, refrigeration.

1. INTRODUCTION

Centrifugal compressors are perhaps the most common example of high-speed turbomachinery. Its applications include aircraft gas turbines, industrial gas turbines, industrial compressors and turbochargers. Constructively the centrifugal compressor is similar to a centrifugal pump. Fluid is drawn in through the inlet casing into eye of the impeller. The function of the impeller is to increase the energy level of the fluid by whirling it outwards, thereby increasing the angular momentum of the fluid. Both the static pressure and the velocity are increased within the impeller. After leaving the impeller section, the fluid enters the diffuser where some of its kinetic energy is converted into pressure. The number of impellers (stages) is directly connected to the required pressure ratio.

The diversity of applications naturally brings about a variety of designs for centrifugal compressors. Although still not available, centrifugal compressors for small refrigeration capacities may be viable with new technological developments. For instance, Reunanen *et al.* (2003) carried out a theoretical analysis, based on an integral formulation, aimed at evaluating the thermodynamic efficiency of centrifugal compressors applied for small capacities (2 kW, 5 kW e 12 kW) for reference test condition LBP and HBP. The authors found out that impellers of small diameter and high speed are required in such applications, raising questions about its feasibility in terms of both manufacture and safe operation. Reunanen *et al.* (2003) called the attention to the crucial importance of refrigerants in centrifugal compressors, since they greatly affect the compressor geometry and operating conditions.

According to Came and Robinson (1999), for many years, impeller aerodynamic design was based on two-dimensional analysis and predominantly empirical. The authors argued that CFD methodologies for three-dimensional simulations has greatly increased the amount of useful data for the design process, with 1D and 2D formulations having their main role in the preliminary phase of design. In fact, the flow in turbomachines is dominated by complex three-dimensional viscous effects, requiring accurate numerical simulation methodologies to allow a precise description of the phenomenon.

Kunz and Lakshiminarayana (1992) have simulated a centrifugal compressor impeller using the turbulence $k-\varepsilon$ model, verifying good agreement between predictions and experimental data. Later, Wang e Komori (1998) developed a methodology to simulate the flow in high speed centrifugal compressors, employing the finite volume approach and the turbulence $k-\varepsilon$ model. More recently, Michael *et al.* (2004) simulated the flow through the geometry of a centrifugal compressor that was experimentally investigated by Eckardt (1975).

The adoption of partial blades or splitters in centrifugal compressors (Fig. 1) is a very common practice but lacks solid design criteria. It is generally recognized, and confirmed in numerous design investigations, that higher mass flow are obtained with splitters, due to a reduction in the slip velocity at the impeller exit and an increase in the effective flow area.

Tang (2006) employed a commercial CFD code to numerically investigate how the splitter positioning affects the performance of small centrifugal impellers. According to the author, for the design flow rate, the compressor performance is improved when the splitter is moved towards the suction side of the blade.

The present study considers a numeric analysis of high speed, low capacity centrifugal compressors designed for HBP (*High Back Pressure*) condition. Results for the three-dimensional flow field are provided to allow the analysis of

the effect of splitters on the compressor thermodynamic efficiency. However, to maintain the computational cost within acceptable bounds, the analysis was only carried out for the first stage of compression.

2. GOVERNING EQUATIONS

The Reynolds-averaged Navier-Stokes equations can be written in the following form:

$$\frac{\partial \rho}{\partial t} + \frac{\partial}{\partial x_i} (\rho U_i) = 0 \quad (1)$$

$$\frac{\partial}{\partial t} (\rho U_i) + \frac{\partial}{\partial x_j} (\rho U_j U_i) = -\frac{\partial P}{\partial x_i} + \frac{\partial}{\partial x_j} \left(\mu \frac{\partial U_i}{\partial x_j} - \overline{\rho u_i u_j} \right) + F_i \quad (2)$$

$$\frac{\partial}{\partial t} (\rho H) + \frac{\partial}{\partial x_j} (U_j \rho H) = \frac{\partial}{\partial x_i} \left(k \frac{\partial T}{\partial x_i} \right) + \frac{\partial P}{\partial t} - \frac{\partial}{\partial x_i} (\overline{\rho u_i h}) \quad (3)$$

In the above equations, $\overline{\rho u_i u_j}$ is the Reynolds stress tensor, which represents the momentum transfer by turbulence, whereas $\overline{\rho u_i h}$ is the turbulent energy flux. The evaluation of values for $\overline{\rho u_i u_j}$ and $\overline{\rho u_i h}$ is the main purpose of turbulence models.

The Reynolds stress tensor is usually expressed according to the Boussinesq hypothesis:

$$-\overline{\rho u_i u_j} = \mu_t \left[\left(\frac{\partial U_i}{\partial x_j} + \frac{\partial U_j}{\partial x_i} \right) - \frac{2}{3} \frac{\partial U_k}{\partial x_k} \delta_{ij} \right] - \frac{2}{3} \rho k \delta_{ij} \quad (4)$$

in which μ_t is the turbulent viscosity.

Similarly, the turbulent energy flux can be represented as a turbulent diffusion, related to μ_t via the definition of a turbulent Prandtl number $Pr_t (= \mu_t C_p / \Gamma_t)$:

$$-\overline{\rho u_i h} = \frac{C_p \mu_t}{Pr_t} \left(\frac{\partial T}{\partial x_i} \right) \quad (5)$$

where C_p represents the specific heat at constant pressure.

The turbulent Prandtl number may have quite different values as a function of the flow condition. According to Wang and Komori (1998), for gas flow the most common adopted value is 0.9. In the present work, sensitivity tests were made with $Pr_t = 0.85$ and 0.90, with no significant difference being noticed. For remaining simulations a value of 0.85 was assumed for Pr_t .

An equation of state for an ideal gas completes the system required to solve the compressible flow through the impeller:

$$\rho = \frac{P}{RT} \quad (6)$$

2.1. Turbulence Modeling

The RNG $k-\varepsilon$ turbulence model (Yakhot and Orzag, 1986) is an improved version of the $k-\varepsilon$ model, derived from the Renormalization Group Theory. Some examples of flows where the RNG $k-\varepsilon$ model has been seen to return better predictions than the standard $k-\varepsilon$ are those including flow separation, streamline curvature and flow stagnation. This explains the superior performance of the RNG $k-\varepsilon$ model for several classes of complex flows, including flows with rotation effects (Yuan *et Al.*, 2003).

Usually, the effective viscosity μ_{ef} is defined as

$$\mu_{ef} = \mu + \mu_t \quad (7)$$

being comprised of the molecular viscosity, μ , and the eddy viscosity, μ_t .

The RNG $k-\varepsilon$ model applied in the present study accounts for rotational effects over turbulence through the following relationship for μ_t :

$$\mu_t = \mu_{t0} f\left(\alpha_s, \Omega, \frac{k}{\varepsilon}\right) \quad (8)$$

where Ω is a characteristic swirl number and α_s is a swirl constant equal to 0.07. For high Reynolds number the eddy viscosity μ_{t0} is calculated from:

$$\mu_{t0} = \rho C_\mu \frac{k^2}{\varepsilon} \quad (9)$$

with $C_\mu = 0.0845$.

The kinetic turbulent energy, k , and the dissipation, ε , necessary to evaluate the turbulent viscosity, are obtained through the following transport equations:

$$\frac{\partial}{\partial t}(\rho k) + \frac{\partial}{\partial x_i}(\rho k u_i) = \frac{\partial}{\partial x_j} \left(\alpha \mu_{ef} \frac{\partial k}{\partial x_j} \right) + \mu_t S^2 - \rho \varepsilon - Y \quad (10)$$

$$\frac{\partial}{\partial t}(\rho \varepsilon) + \frac{\partial}{\partial x_i}(\rho \varepsilon u_i) = \frac{\partial}{\partial x_j} \left(\alpha \mu_{ef} \frac{\partial \varepsilon}{\partial x_j} \right) + C_{\varepsilon 1} \frac{\varepsilon}{k} \mu_t S^2 - C_{\varepsilon 2} \rho \frac{\varepsilon^2}{k} - R \quad (11)$$

where the coefficients $C_{\varepsilon 1}$ and $C_{\varepsilon 2}$ are equals to 1.42 and 1.68, respectively.

The inverse effective Prandtl number, α , in the above equations is determined from:

$$\left| \frac{\alpha - 1,3929}{\alpha_0 - 1,3929} \right|^{0,6321} \left| \frac{\alpha - 2,3929}{\alpha_0 - 2,3929} \right|^{0,3679} = \frac{\mu}{\mu_{ef}} \quad (12)$$

with $\alpha_0 = 1.0$.

The term Y in the Eq. (10) represents the compressible effects of the flow over the turbulence, evaluated in according with the Sarkar and Balakrishnan (1990) purpose:

$$Y = \frac{2\rho \varepsilon k}{\gamma RT} \quad (13)$$

An important term in Eq. (11) is the term R , related to the flow deformation rate and expressed as:

$$R = \frac{C_\mu \eta^3 (1 - \eta / \eta_0) \varepsilon^2}{1 + \beta \eta^3} k \quad (14)$$

where: $\eta = Sk / \varepsilon$; $\eta_0 \cong 4.38$; $\beta = 0.012$; and $S^2 = 2S_{ij}S_{ij}$.

In regions of small strain rate, the term R has a trend to increase μ_t somewhat, but even in this case μ_t still is typically smaller than its value returned by most k - ε models. In regions of elevated strain rate the sign of R becomes negative and μ_t is considerably reduced. This feature of the RNG k - ε is probably the main reason for substantial improvements in the prediction of recirculating flow regions, as compared with other versions of k - ε model.

2.2. Boundary Conditions

Boundary conditions must be prescribed for all dependent variables. With reference to the computational domain (Fig. 1), four types of boundary conditions were adopted in the present study: i) inlet condition (blue surface); ii) outlet condition (yellow surface); iii) solid wall (grey surface); iv) periodical condition (red surface). As can be seen, the inlet boundary condition is located upstream of the impeller inlet, whereas the outlet region is positioned downstream of the impeller outlet.

Evaporation pressure and temperature were imposed as boundary conditions at the inlet. A turbulence intensity of 3% and a turbulence length scale corresponding to the tube hydraulic diameter were adopted as the inlet boundary condition. In the case of backflow at the outlet, temperature and turbulence quantities are evaluated in a similar manner as described for the inlet, otherwise the flow is assumed to be locally parabolic.

At the solid walls all velocity components are zero and an adiabatic condition was assumed. Due to the steep velocity gradients next to the wall surface, non-equilibrium wall functions (Kim and Choudhury, 1995) were adopted to avoid the necessity of solving through the viscous sub-layer. In order to further reduce the computational processing time, only a longitudinal slice of the impeller was included in the solution domain, as depicted in Fig. 1. This was made possible by the use of periodical boundary condition.

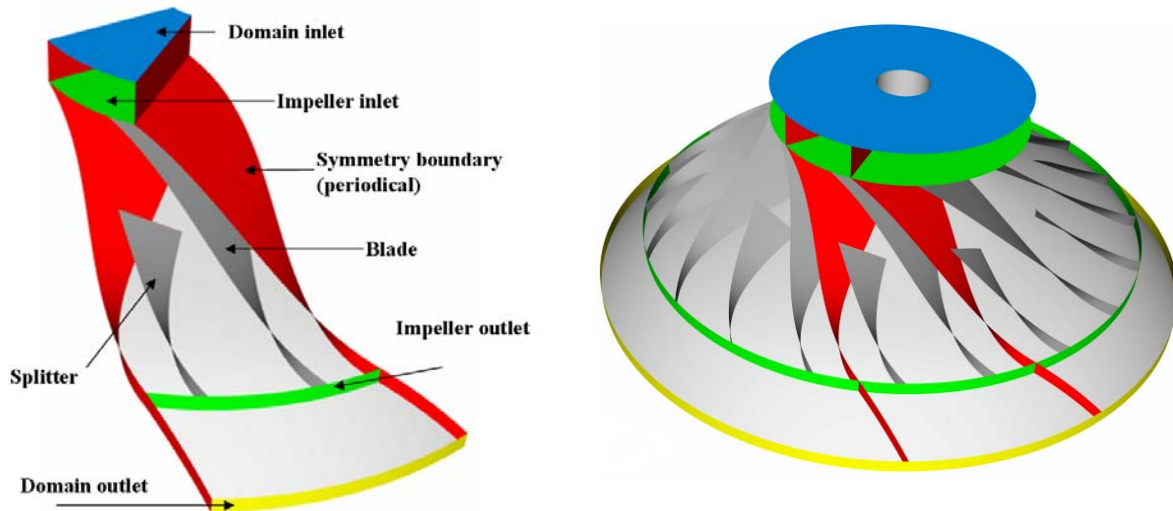


Figure 1. Schematic of the computational domain and boundary surfaces.

3. NUMERICAL SOLUTION PROCEDURE

The numerical simulation of the flow through the compressor impeller was carried out with the commercial code Fluent 6.3.26 (ANSYS, 2006), which is based on the finite volume methodology. The system of algebraic equations was solved with a segregated implicit algorithm. Since the governing equations are not linear, iterative algorithms are applied. Underrelaxation factors are used to reduce numeric instability. PISO algorithm was adopted to solve this pressure-velocity coupled problem, which is suggested for compressible problems (ANSYS, 2006).

A second-order upwind scheme was adopted to interpolate the flow quantities needed at the control volume faces, but for the pressure correction equation the PRESTO! (*PREssure STaggering Option*) scheme was used instead. The PRESTO! scheme provides more accurate interpolations for flow situations in the presence of large body forces or strong pressure variation, such as in swirling flows.

Because the impeller is under rotation, it is convenient to change the reference system and express the governing equations for a rotating solution domain. The main advantage of employing a moving reference frame is to render a problem which is unsteady in the stationary (inertial) frame into a steady condition with respect to the rotating frame.

Due to the inexistence of experimental data for centrifugal compressors of small refrigeration capacities, a very important part of this study was to assess truncation errors by comparing numerical results obtained in grids of different refinements. Based on this analysis of truncation error a tetrahedral mesh with 915.000 volumes was chosen for the numerical simulation of the centrifugal compressor.

4. RESULTS

The main objective of this study is to analyze the effect of splitters on the impeller effective flow area and, as a consequence, on the compressor mass flow rate. The effect of splitters on the thermodynamic efficiency was investigated through the numerical simulation of the flow through the first stage of a two-stage centrifugal compressor, operating with R610a, with a refrigeration capacity of 17.6 kW at HBP condition.

Figure 2 depicts the first stage impeller geometry, with several geometric parameters identified: $r_{1h}= 4.0$ mm; $r_{1l}= 9.65$ mm; $r_2= 38.95$ mm; $b_2= 0.85$ mm. Such quantities were obtained from a preliminary analysis based on an integral approach.

As already mentioned, the design criteria for splitters are not well established. For this reason, in the present work they were positioned equally spaced between two blades. It should be noticed that the length of splitters is shorter than the length of full blades. As pointed out by Tang (2006), the splitter location has an influence on the impeller performance and needs further analysis so as to optimize the compressor efficiency.

One of the main advantages of three-dimensional simulations is the amount of information about the flow phenomena. The analysis of splitters was essentially based on results for pressure and velocity fields, as well as global

quantities such as mass flow rate and pressure ration. All results for flow fields to be presented next are referred to surface situated in a mid plane along the impeller channel, as can be seen in Fig. 2.

Figure 3 demonstrates the great benefit splitters offer in making the velocity field more uniform at the impeller outlet. When splitters are not applied (Fig. 3b) there is a significant velocity gradient at the impeller outlet cross section. This brings about a reduction in the flow slip at the outlet and an increase in the compressor efficiency.

As indicated in Fig. 4, the pressure field is also affected by splitters, reducing the pressure difference between the suction and pressure surfaces. In fact, in the absence of splitters the pressure difference at the impeller outlet reaches approximately 20 kPa.

Table 2 presents a comparison between the performances of impellers with and without splitters. It is evident that the splitters allow an increase in the mass flow rate by nearly 24% in relation to the original design. This higher mass flow rate requires an increase of 6.3% in the torque. However, the torque increase was lower than the mass flow rate increase and the first stage of the compressor stage was raised by 16.8%. The pressure ratio is also increased by almost 4%. Finally, the average tangential velocity at the impeller inlet, $C_{\theta 1}$, was equal to 1.5 m/s in the presence of splitters and 8.0 m/s when splitters were not applied.

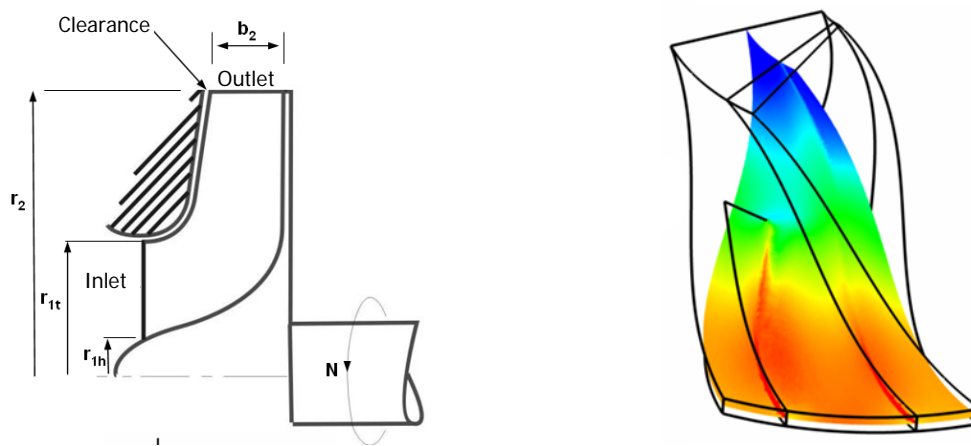


Figure 2. (a) Main geometric parameters and (b) mid plane for flow field results.

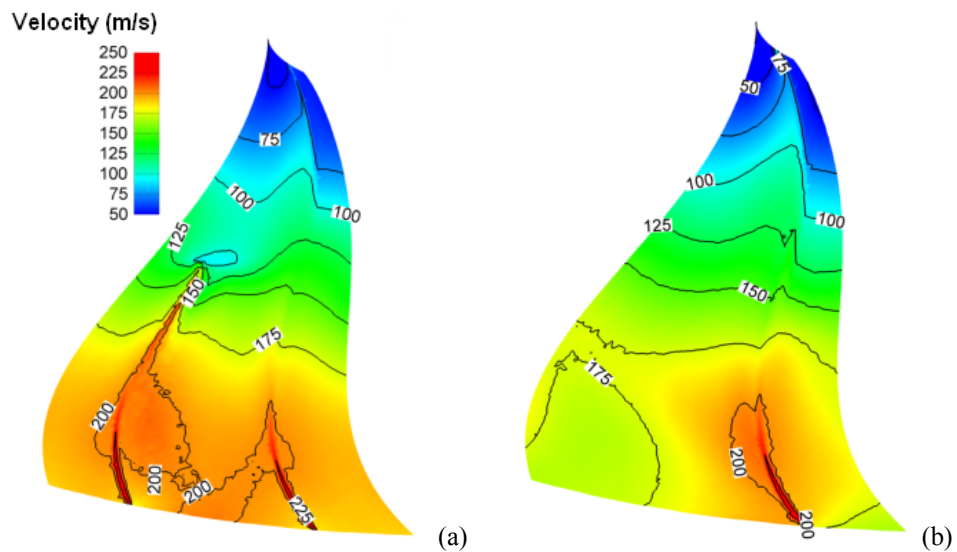


Figure 3. Velocity field in the spanwise direction, (a) impeller with splitters, (b) original impeller.

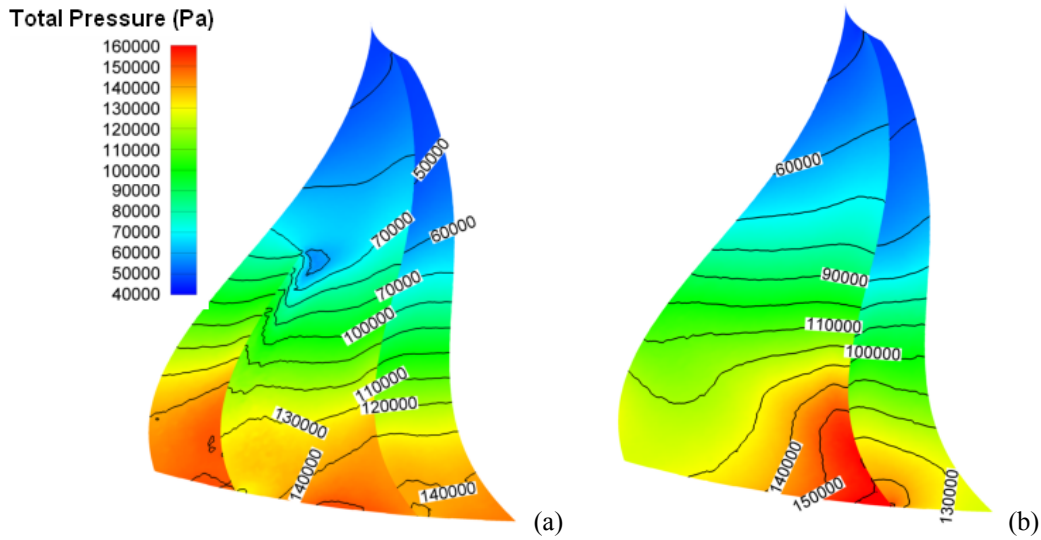


Figure 4. Total pressure field in the spanwise direction, (a) impeller with splitters, (b) original impeller.

Table 2. Results for global parameters of performance.

Case	\dot{m} [g/s]	C_{o2} [m/s]	C_{m2} [m/s]	P_2 [kPa]	P_{o2} [kPa]	P_3 [kPa]
Without splitters	53.1	165.2	46.8	91028	138753	122049
With splitters	65.9	173.2	59.3	89087	144088	124837
Difference	+ 24.2%	+ 4.8%	+ 26.7%	- 2.1%	+ 3.8%	+ 2.3%

5. CONCLUSIONS

The present study considered the numerical simulation of the three-dimensional flow through the impeller of a high speed centrifugal compressor to verify the effect of splitters on the compressor thermodynamic efficiency. The account for turbulence effects in the flow was accomplished by using the RNG $k-\varepsilon$ turbulence model. The governing equations were numerical solved via the volume finite methodology. Due to the unavailability of experimental data for centrifugal compressors of small refrigeration capacities as considered in the present work, a systematic analysis of truncation error was included. The numerical simulations were carried out for the first stage of a centrifugal compressor with a refrigeration capacity of 17.6 kW, at HBP test condition. Results for velocity and pressure fields in the impeller, with and without splitters, has clearly demonstrated the benefit of adopting splitters in the compressor design. The more uniform flow condition at the impeller outlet allowed an increase in the mass flow rate of approximately 24%.

6. ACKNOWLEDGEMENTS

This study is part of a technical-scientific program between the Federal University of Santa Catarina and EMBRACO. Support from FINEP (Federal Agency of Research and Projects Financing) and CAPES (Coordination for the Improvement of High Level Personnel) is also acknowledged.

7. REFERENCES

- Ansyes Inc., Fluent, Version 6.3.26, USA, 2006.
- Barth, T. J., and Jespersen, D., The Design and Application of Upwind Schemes on Unstructured Meshes, Technical Report AIAA-89-0366, AIAA 27th Aerospace Sciences Meeting, Reno, Nevada, USA, 1989.
- Came, P. M., and Robinson, C. J., Centrifugal Compressor Desing, ImechE, Proc. Instn. Mech. Engrs. Vol. 213, Part C, 139-155, 1999.
- Kim, S. E., and Choudhury. D. A Near-Wall Treatment Using Wall Functions Sensitized to Pressure Gradient, ASME, Separated and Complex Flows, Vol. 217, 1995.

- Kunz, R. F., and Lakshminarayana, B., Three-Dimensional Navier-Stokes Computation of Turbomachinery Flows Using an Explicit Numerical Procedure and a Coupled k - ϵ Turbulence Model, *Journal of Turbomachinery*, Vol. 114, 627-642, 1992.
- Reunanen, A., Honkatukia, J., Kuosa, M., Larjola, J., Theoretical Evaluation of Centrifugal Compressors for Cooling Purposes Using Existing Refrigerants, Technical Report LFD6, Lappeeranta University of Technology, Finland, 2003.
- Sarkar, S., and Balakrishnan, L., Application of a Reynolds-Stress Turbulence Model to the Compressible Shear Layer, ICASE Report 90-18, NASA CR 182002, USA, 1990.
- Tang, J., Computational Analysis and Optimization of Real Gas Flow in Small Centrifugal Compressors, Lappeeranta University of Technology, Finland, 2006.
- Yakhot, V., and Orzag, S. A., Renormalization Group of Turbulence. Basic Theory, *J. Sci. Comput.*, Vol. 1, 3-51, 1986.
- Yuan, Z. X., Saniei, N. and Yan, X. T., Turbulent Heat Transfer on the Stationary Disk in a Rotor-Stator System, Elsevier Science, *Int. J. of Heat and Mass Transfer.*, Vol. 46, 2207-2218, 2003.
- Wang, Y., and Komori, S., Simulation of the Subsonic Flow in a High-Speed Centrifugal Compressor Impeller by the Pressure-Based Method, *ImechE, Proc. Instn. Mech. Engrs.* Vol. 212, Part A, 269-287, 1998.

8. RESPONSIBILITY NOTICE

The authors are the only responsible for the printed material included in this paper.